

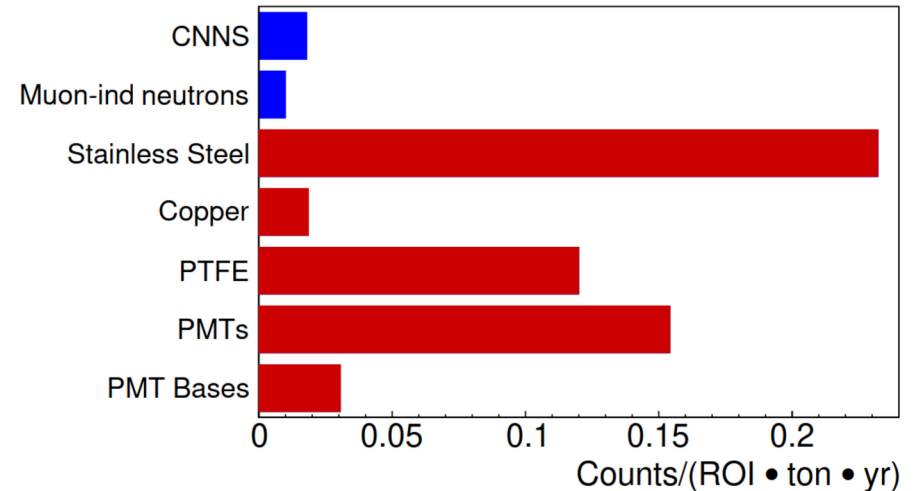
The low-background germanium counting facility Gator for high-sensitivity γ -ray spectrometry

Zurich PhD Student Seminar

Alexander Bismark
(alexander.bismark@physik.uzh.ch)
26 January 2023

Motivation

- Required low backgrounds in rare event searches (e.g. DM, $0\nu\beta\beta$)
- Germanium spectroscopy: non-destructive and high resolution screening method for material radioassay
- Selection of radiopure detector materials and precise background simulations
- Gator facility used for...
 - XENON100, XENON1T and XENONnT, GERDA and LEGEND-200
 - Future: LEGEND-1000 and DARWIN



Nuclear recoil backgrounds in XENON1T from materials (red), predicted from screening measurements, and external sources (blue)^[1]

[1] Eur. Phys. J. C77 (2017) 890

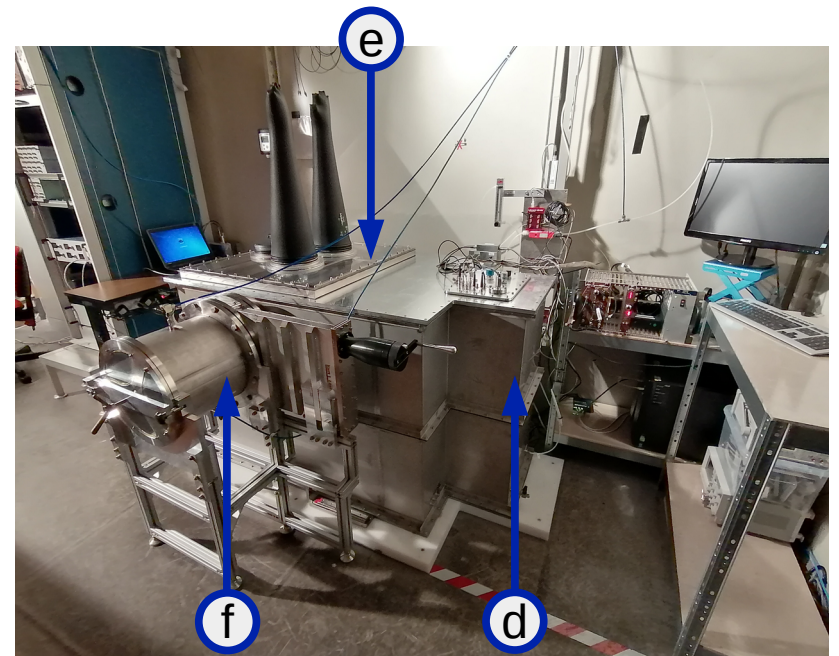
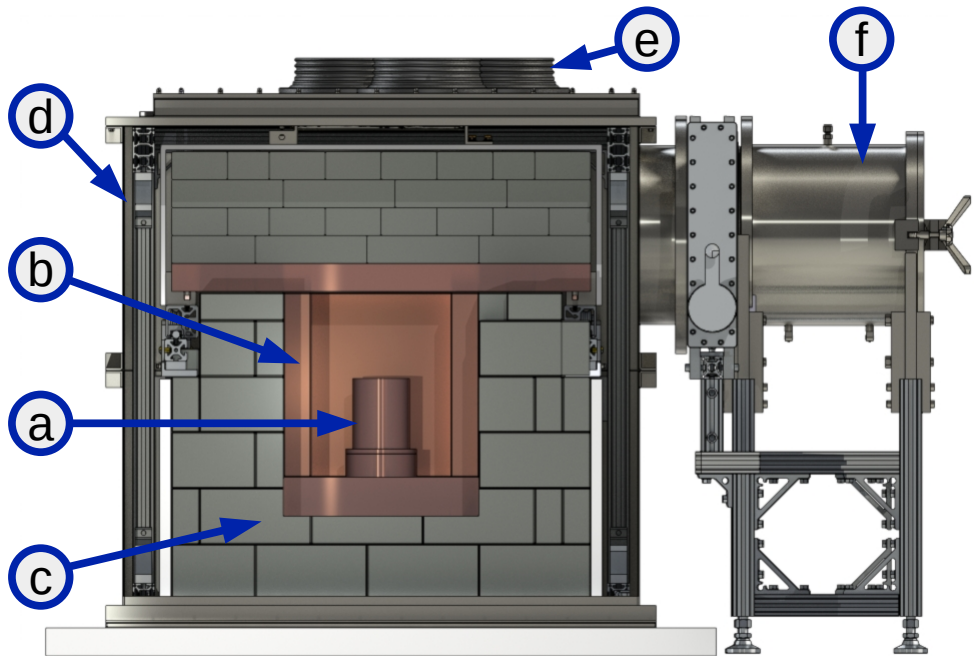
The Gator Facility

- Low-background germanium counting facility for high-sensitivity γ -ray spectrometry^[2]
- Located at the Gran Sasso underground laboratory in Italy (LNGS) at a depth of 3600 m water equivalent
- Core: p-type coaxial high-purity germanium (HPGe) detector with 2.2 kg sensitive mass and a relative efficiency of 100.5%
- Sample chamber volume: $25 \times 25 \times 33 \text{ cm}^3$
- Recent upgrades to decrease background level, noise contribution in low-energy region, facilitate sample handling process



[2] JINST 17 (2022) P08010

The Upgraded Gator Detector



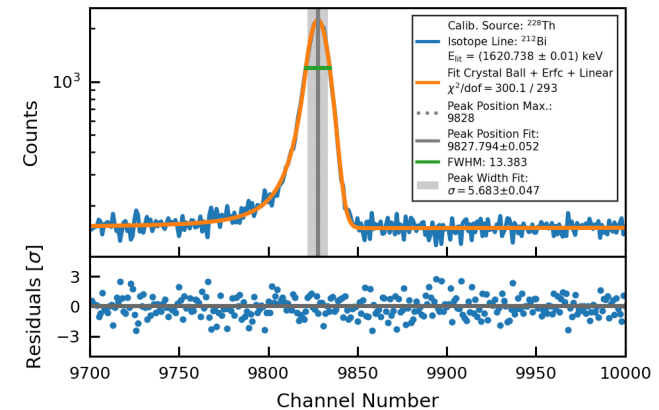
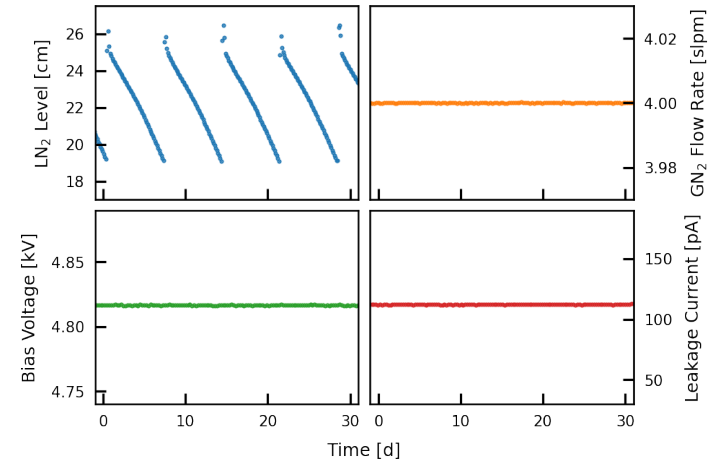
(a) HPGe detector inside Cu-OFE cryostat (cooled with LN₂ via copper coldfinger), **(b)** OFHC Cu cavity, **(c)** lead shield, polyethylene sheet, **(d)** airtight stainless steel enclosure (purged with GN₂), **(e)** glove ports, **(f)** sample load lock

Detector Operation and Performance

- Stable operation for over 10 years
- Remote monitoring (incl. alarms) of operations parameters to ensure detector stability and data quality
- Regular calibrations of the detector with radioactive sources (e.g. ^{228}Th , ^{137}Cs , or ^{60}Co) or high-activity samples
 - FWHM at 1332 keV: (1.98 ± 0.07) keV (Maeve: 3.19 keV^[3], GeOroel: 1.85 keV^[4])
 - Verification of simulated efficiencies and consistent activities related lines

[3] Eur. Phys. J. C80 (2020) 1044

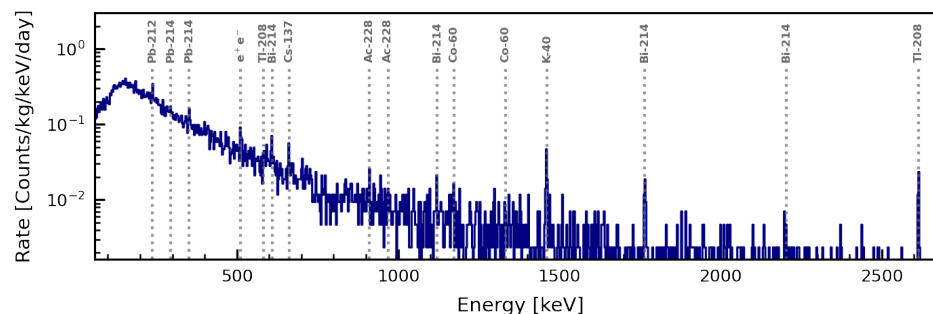
[4] Bandac, "Ultra-Low Background Services in the LSC", DS-Mat Meeting, GSSI, 2019



Background Contributions

- Integrated background rate in the energy region 100-2700 keV ^[2]:
 $(82.0 \pm 0.7) \text{ d}^{-1} \text{ kg}^{-1}$;
 as compared to value from 2010 ^[5]:
 $(102.8 \pm 0.7) \text{ d}^{-1} \text{ kg}^{-1}$;
 stable within runs ($\chi^2/\text{ndf} \approx 1$)
- Low energies ($\lesssim 35 \text{ keV}$, below ROI):
 - electronic noise
- Higher energies:
 - detector & shielding materials
 - environmental radon

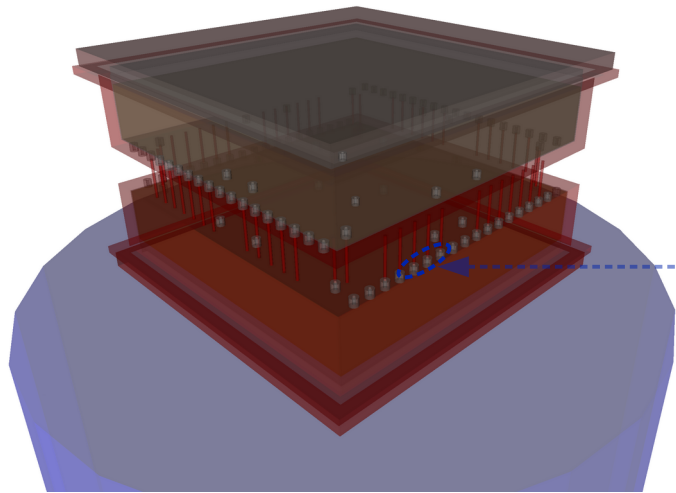
Energy [keV]	Isotope	Rate '21 [d^{-1}]	Rate '10 [d^{-1}]
351.932	Pb-214	0.41 ± 0.17	0.7 ± 0.3
609.312	Bi-214	0.26 ± 0.10	0.6 ± 0.2
1120.29	Bi-214	< 0.28	0.3 ± 0.1
1764.49	Bi-214	0.14 ± 0.06	0.08 ± 0.06
661.657	Cs-137	0.19 ± 0.09	0.3 ± 0.1
1173.24	Co-60	< 0.27	0.5 ± 0.1
1332.51	Co-60	< 0.21	0.5 ± 0.1
1460.88	K-40	0.28 ± 0.08	0.5 ± 0.1
2614.51	Tl-208	0.19 ± 0.05	0.2 ± 0.1



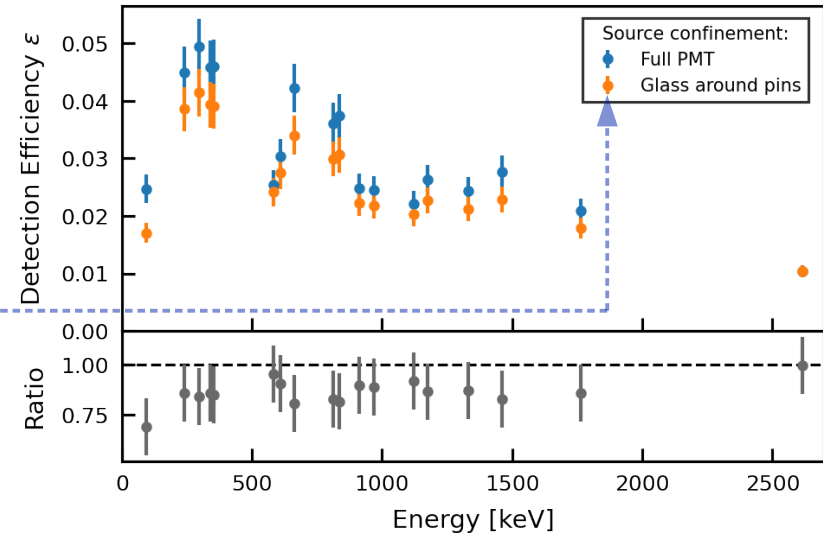
[2] JINST 17 (2022) P08010, [5] JINST 6 (2011) P08010

Sample Simulation and Analysis

- Determination of the material-, geometry-, and energy-dependent detection efficiency ϵ of the respective γ -lines through GEANT4 Monte Carlo simulations for each sample



Simulated R12699 PMTs on detector



Resulting detection efficiencies lines

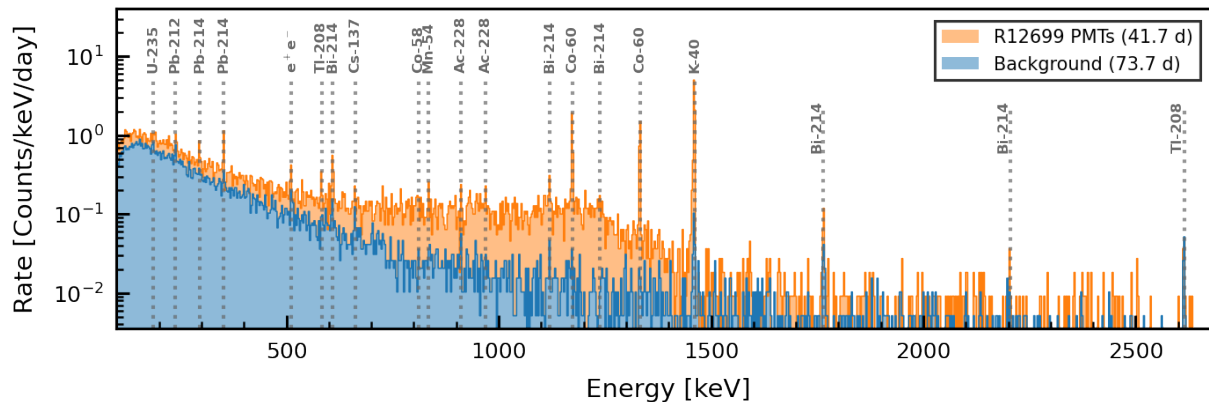
Sample Simulation and Analysis

- Calculation of the specific activities A from the background- and Compton-subtracted counts S_{net} at the location ($\pm 3\sigma$) of the most prominent lines as

$$A = \frac{S_{net}}{r \cdot \epsilon \cdot m \cdot t}$$

(branching ratio r , sample mass m , measuring time t)

- Combination to activities of isotopes / subchains (L_d @ 90% C.L.)



$$S_{net} = S - B \cdot \frac{t_S}{t_B} - B_C$$

$$L_d = k^2 + 2 \cdot L_c$$

$$L_c = k \cdot \sigma_{net} \quad [6]$$

[6] Anal. Chem. 1968, 40, 3, 586–593

Example: Hamamatsu PMT R12699-406-M4

For isotopes where detection limit is exceeded, current PMT model (still being optimized) has, per active photocathode area*,

- tenth – fourfold activities w.r.t. R11410 units (in XENON1/nT) [1]
- lower activity compared to the R8520 PMTs (in XENON100) [5]

→ Good potential for future improvements through material selection for use in DARWIN

* R12699 ~ 23.5 cm², R11410 ~ 32.2 cm², R8520 ~ 4.2 cm²

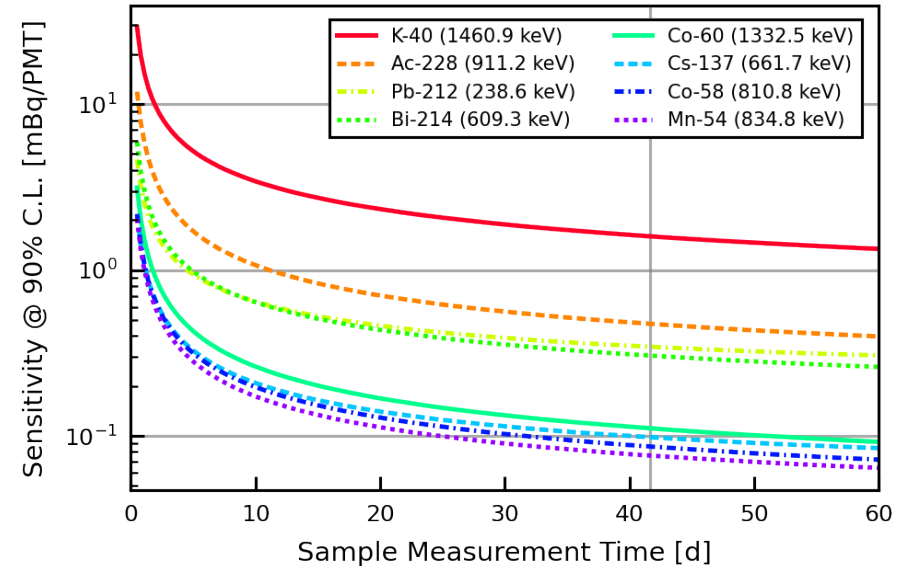
Isotope	Confinement full PMT				
	Improved LRI model	Initial model	Prototype Screening 2018	Hamamatsu R11410	Hamamatsu R8520-06
Detected/Limit (90 % C.L.) Activity [mBq/PMT]					
²³⁸ U	< 6.92	< 6.11	< 8.13	8 ± 2	< 15
²²⁶ Ra	0.54 ± 0.09	0.60 ± 0.10	0.54 ± 0.21	0.6 ± 0.1	< 0.28
²²⁸ Ra	< 0.55	< 0.65	< 0.95	0.7 ± 0.2	< 0.59
²²⁸ Th	< 0.36	< 0.53	0.49 ± 0.2	0.6 ± 0.1	0.3 ± 0.1
²³⁵ U	< 0.32 [< 6.43]	< 0.28 [< 5.66]	< 0.37 [< 9.51]	0.37 ± 0.09	< 0.67
⁶⁰ Co	0.08 ± 0.04	1.31 ± 0.11	2.02 ± 0.19	0.84 ± 0.09	0.60 ± 0.04
⁴⁰ K	34.2 ± 3.6	34.6 ± 3.7	26.3 ± 3.2	12 ± 2	12.0 ± 0.8
¹³⁷ Cs	< 0.113	< 0.119	0.151 ± 0.058	–	< 0.1
⁵⁴ Mn	0.17 ± 0.04	< 0.146	< 0.189	–	–
⁵⁸ Co	0.24 ± 0.04	< 0.122	< 0.222	–	–
Detected/Limit (90 % C.L.) Activity [mBq/cm ²]					
²³⁸ U	< 0.294	< 0.260	< 0.346	0.25 ± 0.06	< 3.569
²²⁶ Ra	0.023 ± 0.004	0.026 ± 0.004	0.023 ± 0.009	0.019 ± 0.003	< 0.067
²²⁸ Ra	< 0.023	< 0.028	< 0.040	0.022 ± 0.006	< 0.140
²²⁸ Th	< 0.015	< 0.023	0.021 ± 0.009	0.019 ± 0.003	0.071 ± 0.017
²³⁵ U	< 0.014 [< 0.273]	< 0.012 [< 0.241]	< 0.016 [< 0.404]	0.012 ± 0.003	< 0.159
⁶⁰ Co	0.0036 ± 0.0016	0.055 ± 0.005	0.086 ± 0.008	0.026 ± 0.003	0.144 ± 0.010
⁴⁰ K	1.45 ± 0.15	1.47 ± 0.16	1.12 ± 0.14	0.37 ± 0.06	2.86 ± 0.18
¹³⁷ Cs	< 0.005	< 0.005	0.006 ± 0.002	–	< 0.024
⁵⁴ Mn	0.0070 ± 0.0015	< 0.006	< 0.008	–	–
⁵⁸ Co	0.0103 ± 0.0018	< 0.005	< 0.009	–	–

[1] Eur. Phys. J. C77 (2017) 890; [7] Astropart. Phys. 35 (2011) 43–49

Sample Simulation and Analysis

- Isotopes / chains of interest:
 - primordial: ^{238}U , ^{232}Th , ^{40}K
 - cosmogenic: ^{54}Mn , ^{46}Sc , ^{60}Co , ...
 - anthropogenic: ^{137}Cs , $^{110\text{m}}\text{Ag}$, ...

→ decay products may mimic signals or leak into the signal region
- Typical sensitivities: < a few **mBq/kg** for exposures of 1-3 weeks and several kg sample mass (a few **$\mu\text{Bq/kg}$** for radio-pure samples, longer exposure and higher mass)



2 Hamamatsu R12699-406-M4 PMTs

Comparison to Other HPGe Spectrometers

Detector	Location (Depth m.w.e.)	Mass [kg]	Efficiency [%]	FWHM [keV]	Rate 60-2700 keV [cnts/(kg·day)]	Ref.
Gator	LNGS (3600)	2.2	100.5	1.98	89.0 ± 0.7	[2]
Maeve	SURF (4300)	2.0	85	3.19	956.1	[3]
GeMPI 3	LNGS (3600)	2.2	98.7	2.20	24 ± 1	[8]
Belmont	Boulby (2805)	3.2	160	1.92	135.0	[3]
GeOroel	LSC (2450)	2.3	109	1.85	165.3	[4]
GeMSE	LVdA (620)	2.0	107.7	1.96	88 ± 1	[9]

[2] JINST 17 (2022) P08010

[3] Eur. Phys. J. C80 (2020) 1044

[4] Bandac, "Ultra-Low Background Services in the LSC", DS-Mat Meeting, GSSI, 2019

[8] N. Ackermann, private communication

[9] JINST 17 (2022) P04005

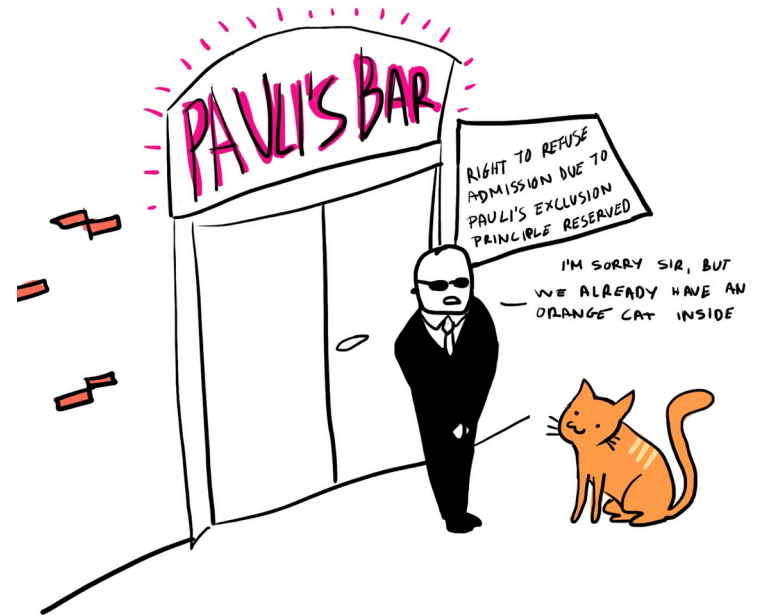
Tests of the Pauli-Exclusion-Principle (PEP)

- Two or more identical fermions cannot occupy the same quantum state within a quantum system simultaneously
- Messiah–Greenberg Superselection Rule**

The symmetry of the wave function of a steady state is constant in time

→ the symmetry of a quantum state can only change if a particle, which is new to the system, interacts with the state

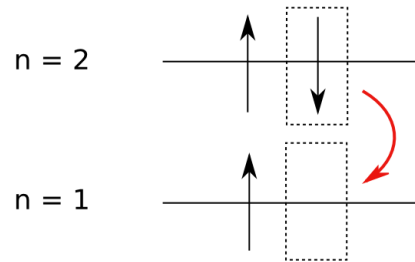
- Categorize PEP violation experiments by the “novelty” of the fermion-system interaction



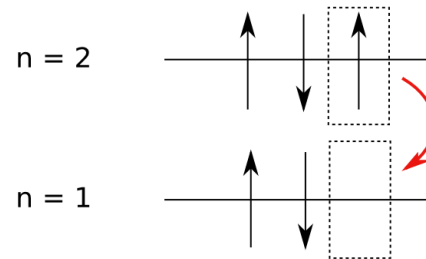
Ramberg-Snow Technique

- Search for PEP forbidden atomic transitions
- Type II: electrons from external current
 - fermion has not previously interacted with the investigated system
- Here: current through Pb
 - e.g., $1s-2p_{3/2}$ $K_{\alpha 1}$:
74.961 keV (allowed) /
73.713 keV (forbidden)

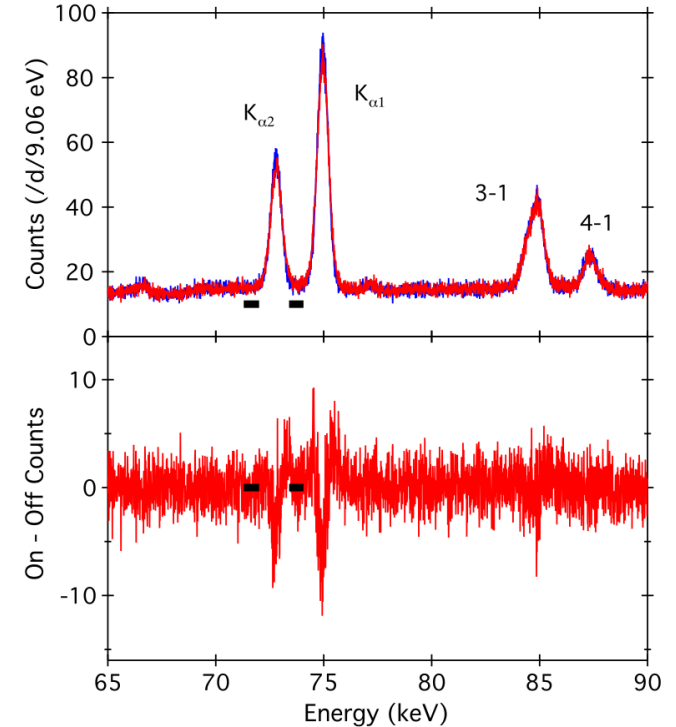
Normal...



Non-Paulian...



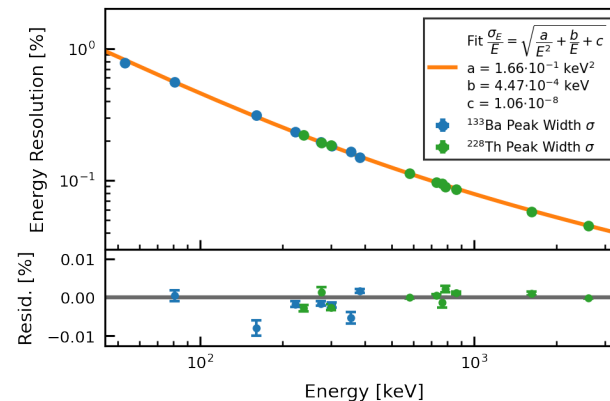
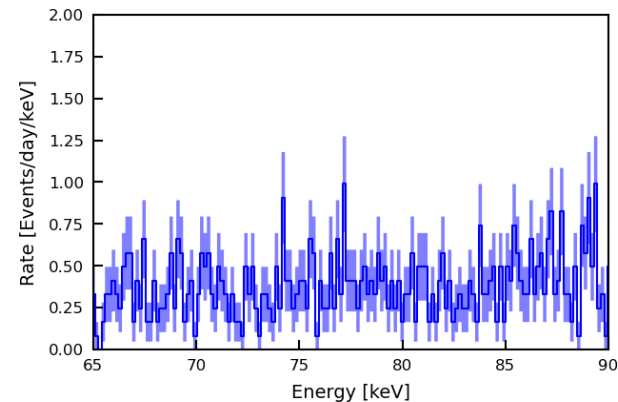
atomic $2p - 1s$ transition



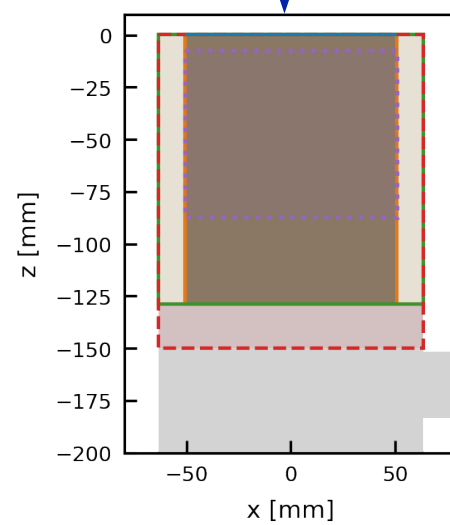
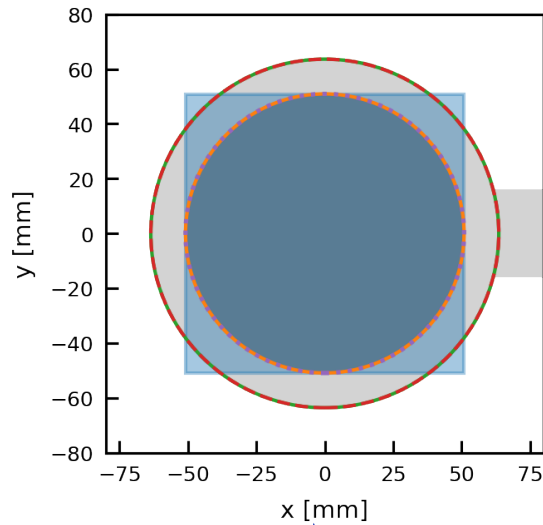
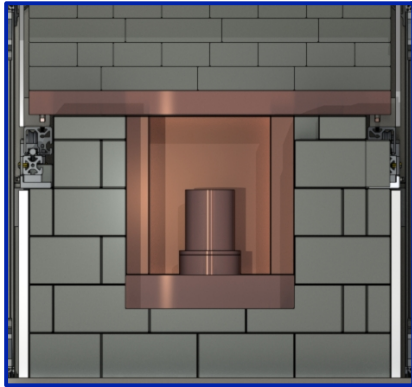
[10] Found Phys 42, 1015–1030 (2012)

PEP Studies in Gator

- Integrated background rate in the ROI (65-90 keV): $(4.4 \pm 0.3) \text{ d}^{-1} \text{ kg}^{-1}$
- Resolution (FWHM) at 74.96 keV: $\sim 1.05 \text{ keV}$
- Low activity material selection based on previous screenings or new measurements on demand
 - Roman Pb sheets from Lemer Pax with $< 0.2 \text{ Bq/kg}$
 - OFHC copper and PTFE for support from XENON experiments
 - High current cables currently being screened
- Aim for currents up to 180 A (first step: 100 A)



Simulations – Investigated Geometries Pb Conductor

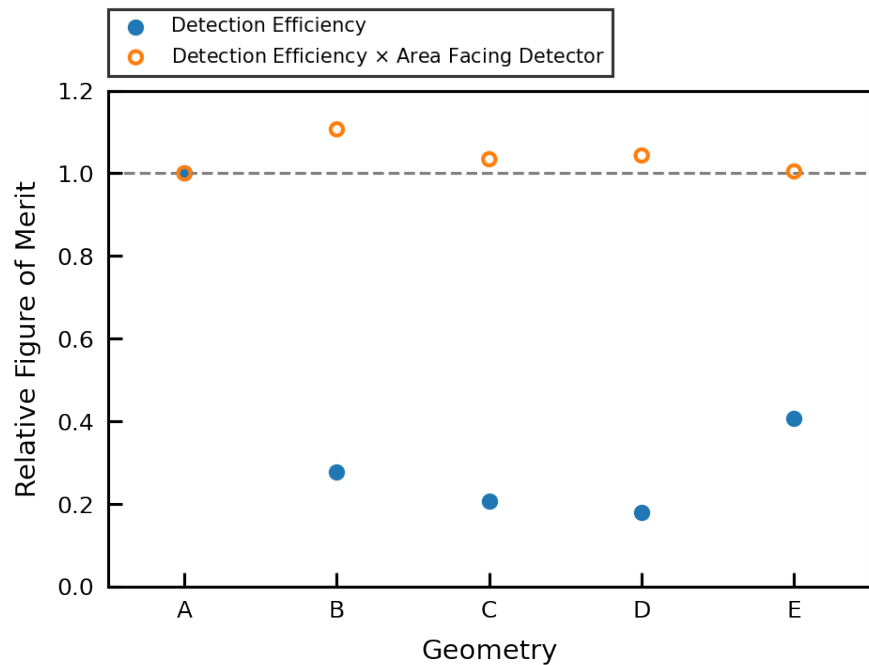


- Cu Cryostat Endcap:
 $D_{outer} = 101.6 \text{ mm}$
 $\Delta z = 129.05 \text{ mm}$
- Cu Cryostat Base (+ Coldfinger):
 $D_{outer} = 127.0 \text{ mm}$
- Hollow Cylinder:**
 $D_{inner} = 101.8 \text{ mm}$
 $\Delta z = 129.05 \text{ mm}$
- Hollow Cylinder:
 $D_{inner} = 127.2 \text{ mm}$
 $\Delta z = 129.05 \text{ mm}$
- Hollow Cylinder:
 $D_{inner} = 127.2 \text{ mm}$
 $\Delta z = 150.0 \text{ mm}$
- Hollow Cylinder:
 $D_{inner} = 127.2 \text{ mm}$
 $\Delta z = 79.8 \text{ mm}$
 (Sensitive Vol. Sim.)
- Plate:**
 $\Delta x = \Delta y = 101.6 \text{ mm}$

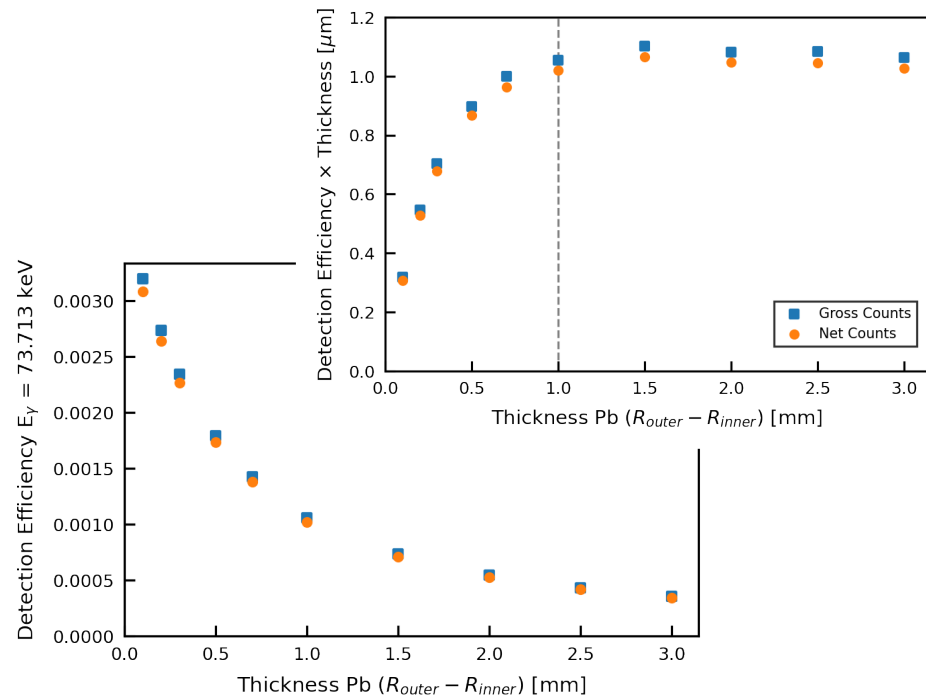
- B
- C
- D
- E
- A

Detection Efficiency

Geometries

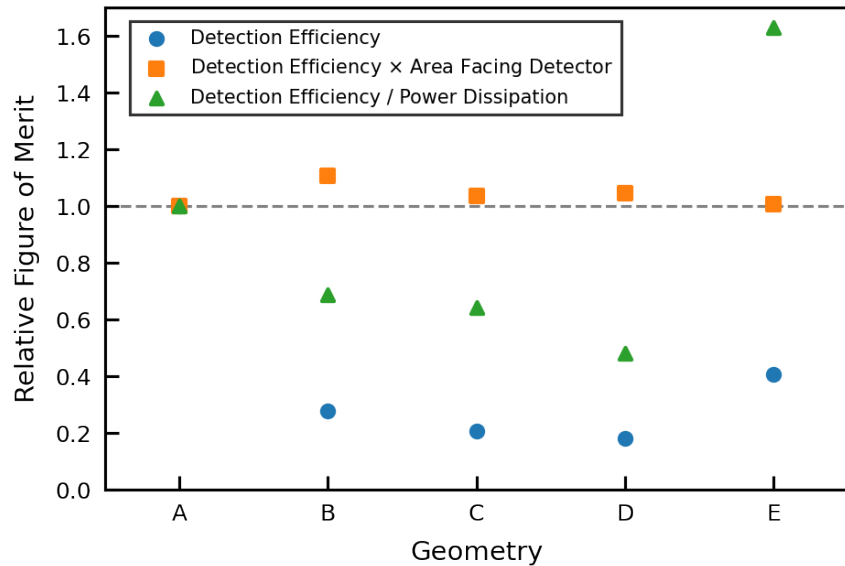


Thickness (Geom. D)

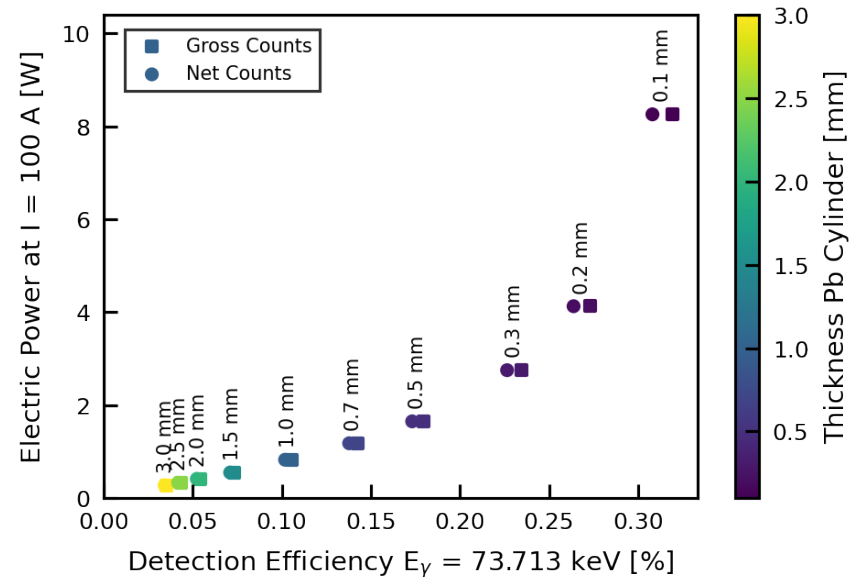


Power Dissipation

Geometries

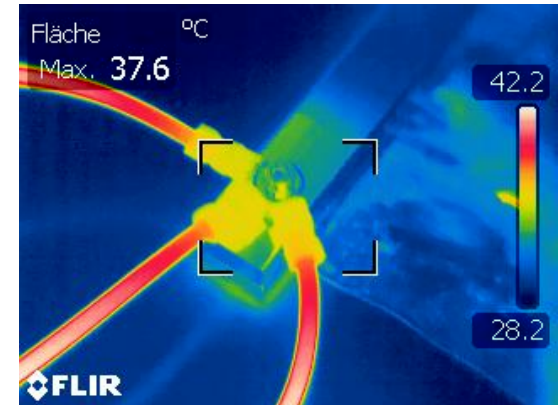
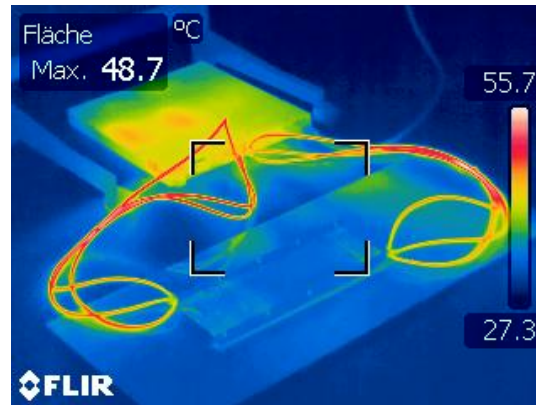
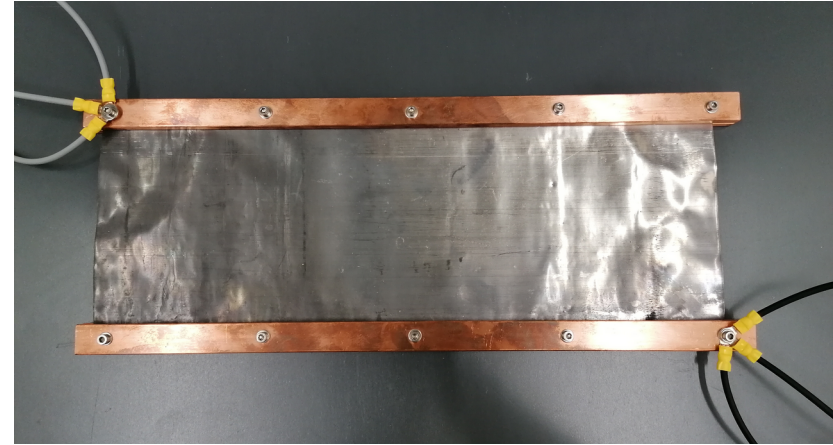
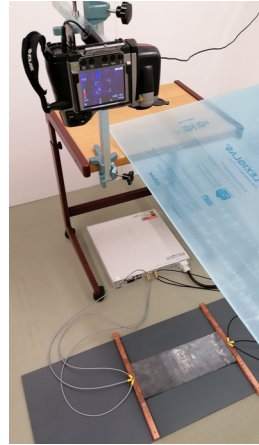


Thickness (Geom. D)

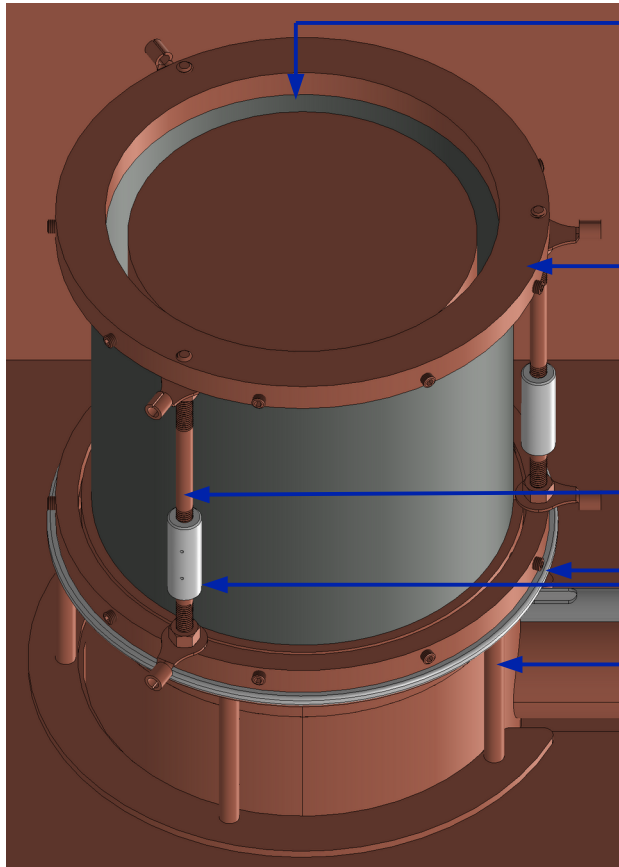


Heat-Up Tests

- Heat dissipation tests with flat geometry in 2 configurations for $42 \times 14.7 \times 0.05 \text{ cm}^3$ Pb sheet (estimate 1.4 / 12.1 W Pb only)
- Currents up to 100 A, clamped in Cu bars ($\varnothing 2 \times 1.6 \text{ cm}^2$, $\rho_{\text{Cu}} \approx 0.08 \rho_{\text{Pb}}$), 27-28°C ambient temperature
- Significant heat-up of $3 \times 4 \text{ mm}^2$ cables (estimate 32 W, resulting in increased R), Pb sheet / Cu bars mostly unaffected



Setup Design



Pb foil cylinder:
 $h = (108 + 2 \times 6) \text{ mm}$
 $D_{\text{inner}} = 121.6 \text{ mm}$
→ 1 cm to cryostat

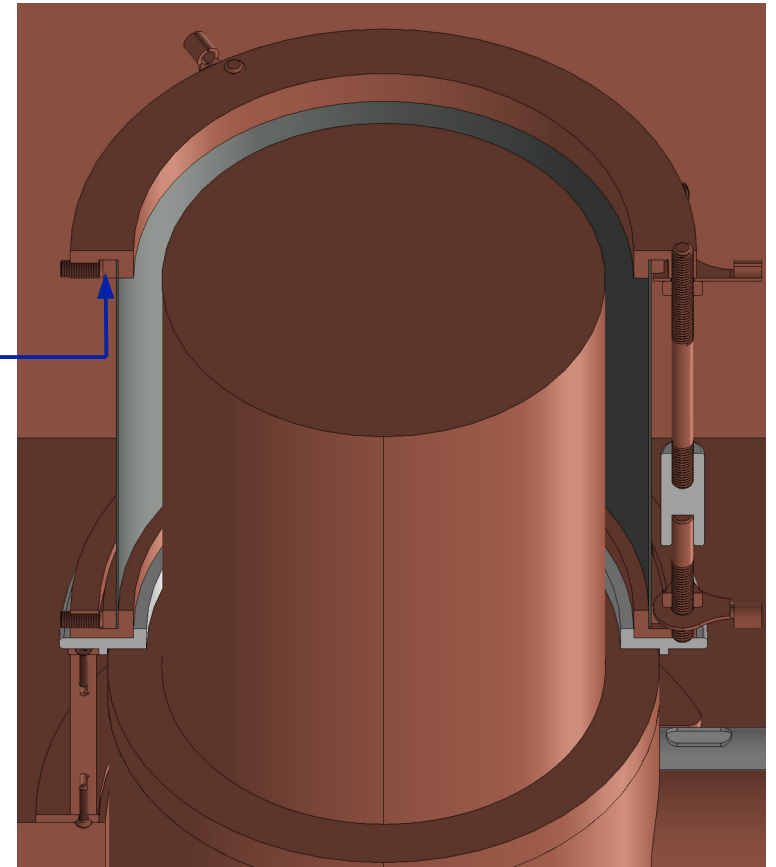
Cu rings for el. contact
Segmented Cu clamps
+ set screws

Cu support rods

PTFE insulators

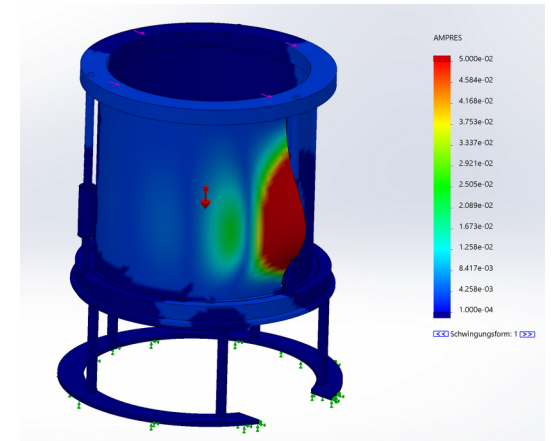
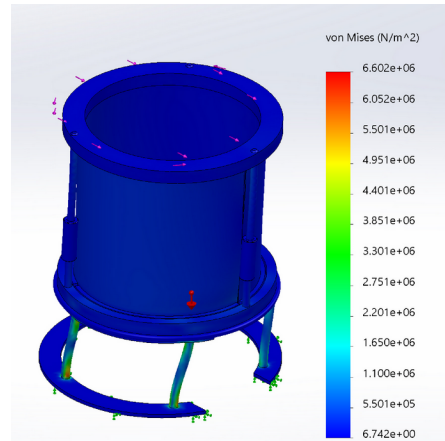
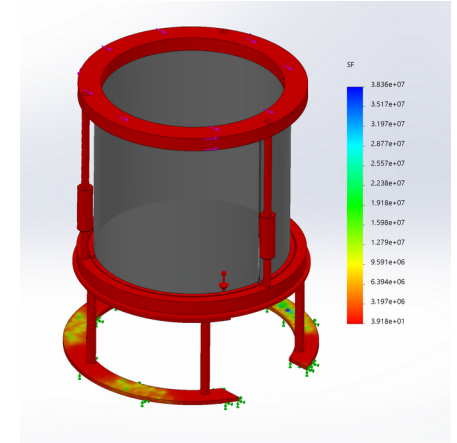
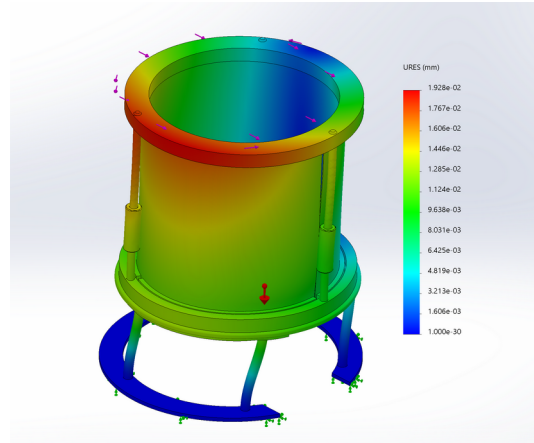
Cu pedestal

Trade-off low activity
(~mass, total ca. 1.5 kg)
↔ low R & high stability



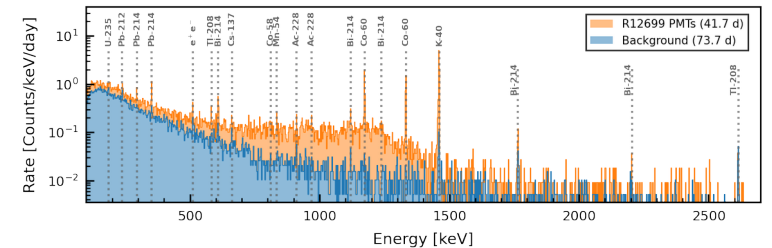
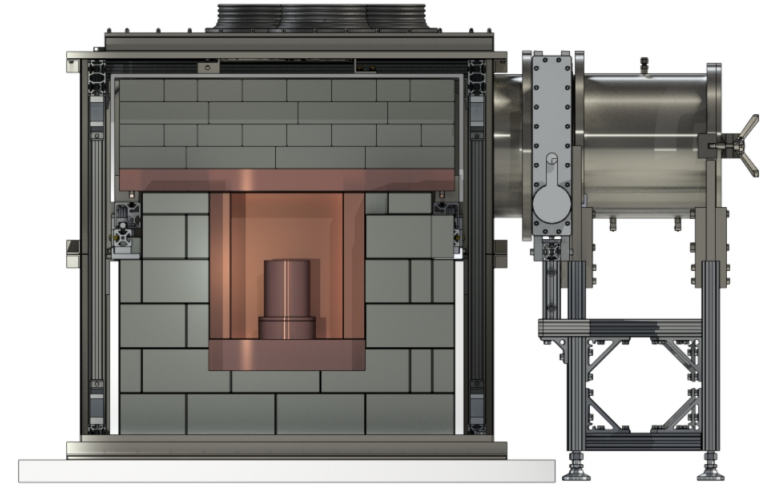
Stability Simulations

- SolidWorks stability simulations: static (stress, displacement, strain, safety factor) + buckling
- Gravity + different force / torque scenarios (shown: extreme case, i.e. gravity + 10 N lateral force top + 1 Nm torque)
- Minimum safety factor:
 - 570 (gravity only)
 - 39 (extreme case)

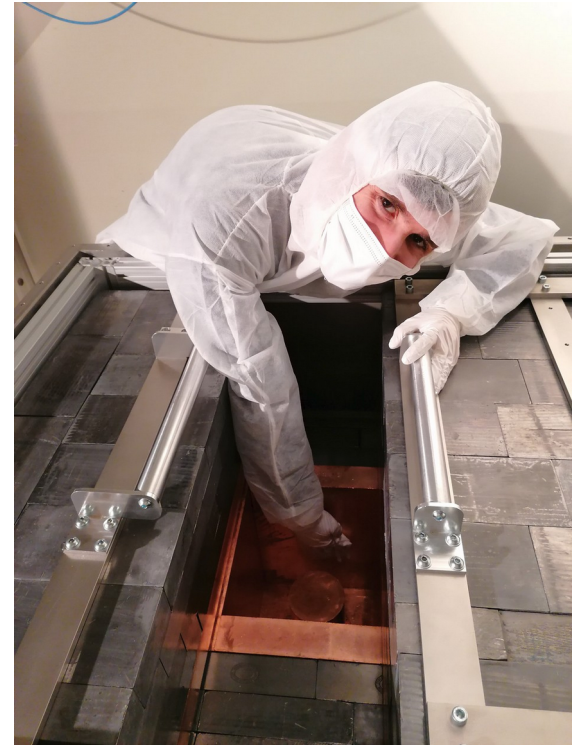


Summary and Outlook

- Low-background germanium counting facility Gator for high-sensitivity gamma-ray spectrometry
- Integrated background rate (100-2700 keV) of $(82.0 \pm 0.7) \text{ d}^{-1} \text{ kg}^{-1}$ comparable to world's most sensitive HPGe detectors
- Prospective material screenings for LEGEND-1000, DARWIN,...
- Search for Pauli-Exclusion-Principle forbidden atomic transitions in lead

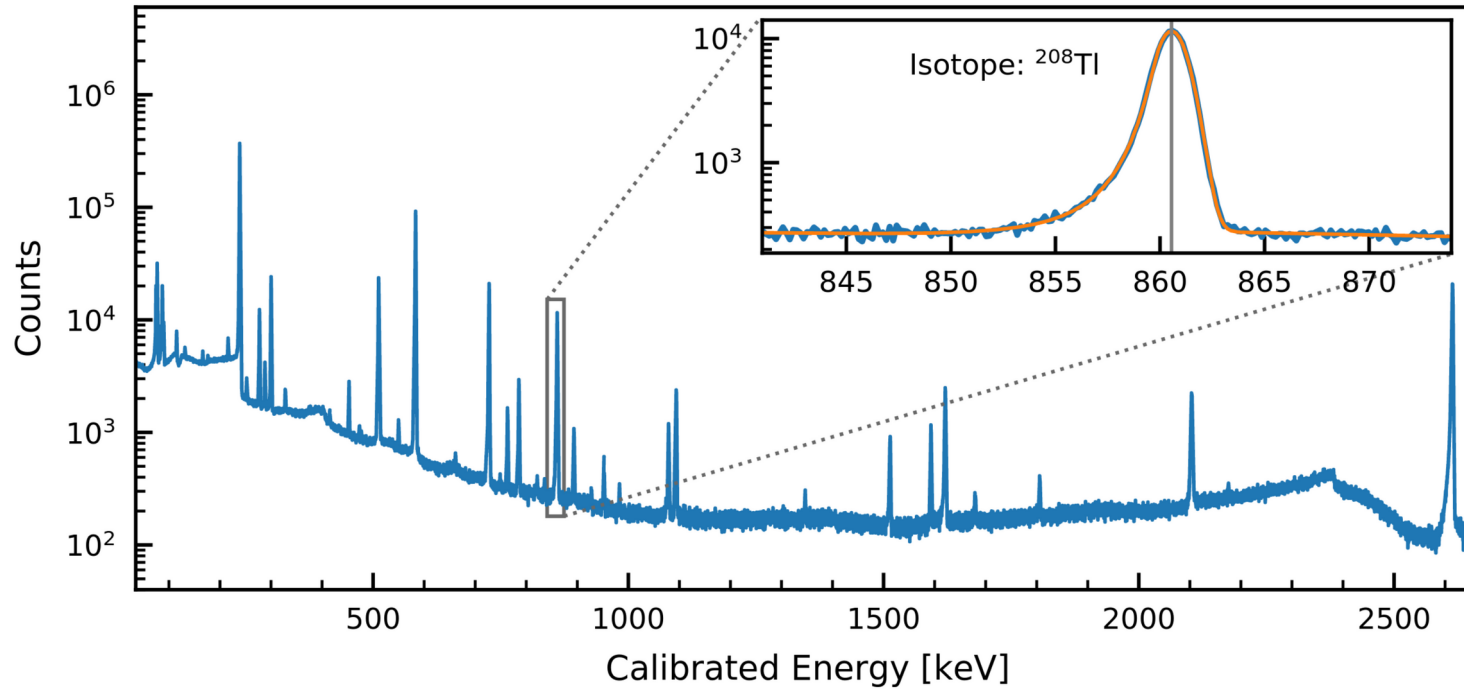


Thank you for
your attention!
Questions?



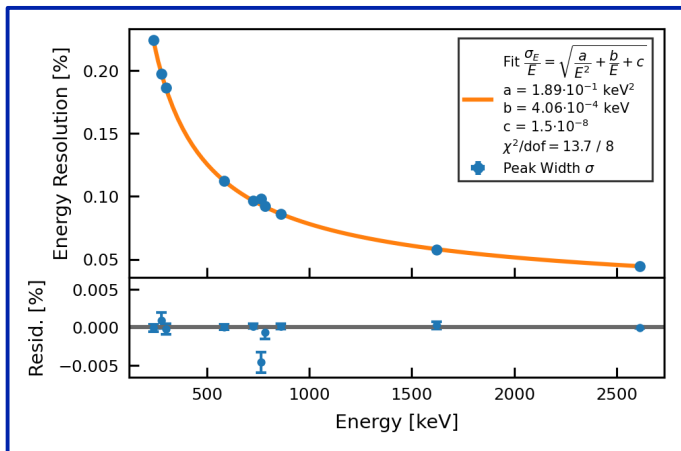
Appendix

Calibration Example: Th-228

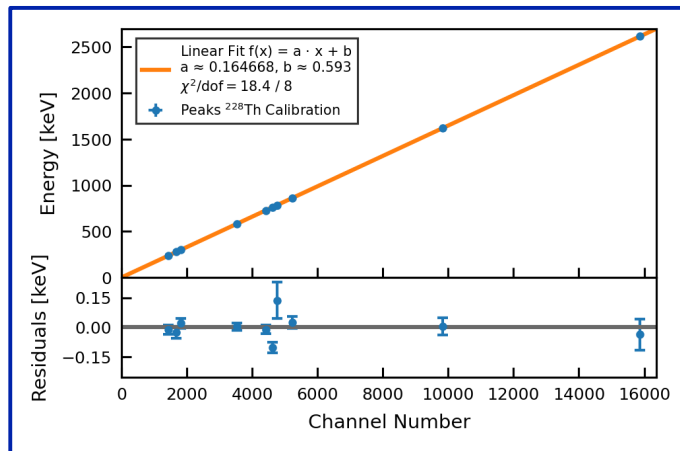


Calibration Example: Th-228

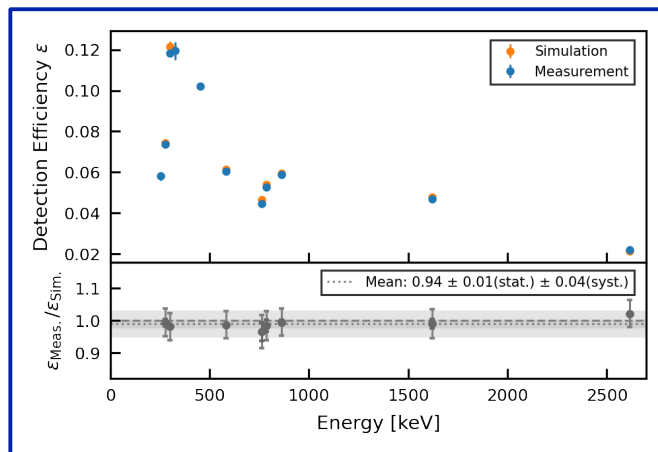
Energy resolution



Linearity

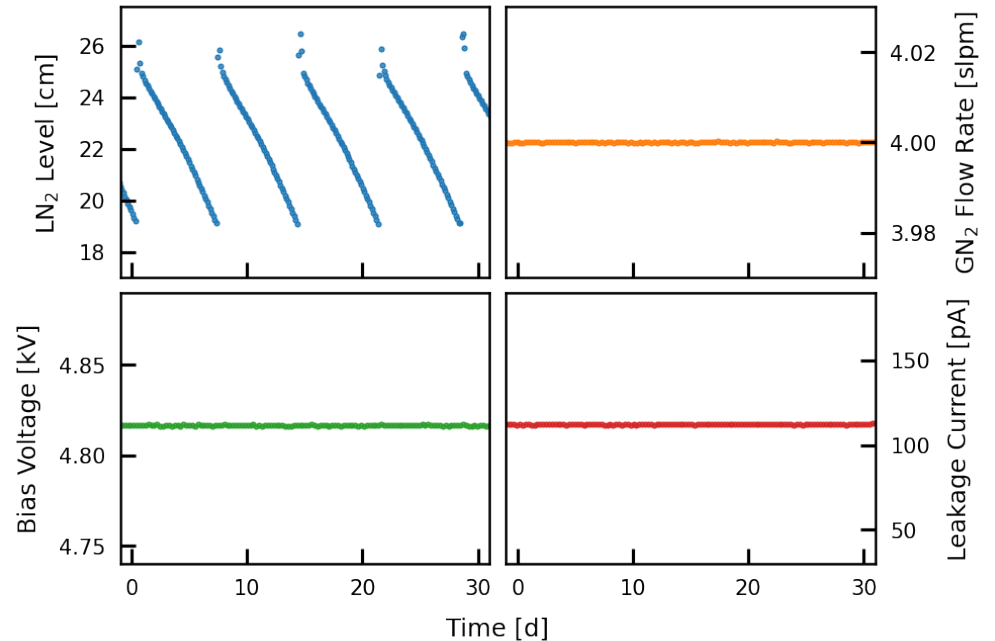


Verification Sim.
Det. Efficiency



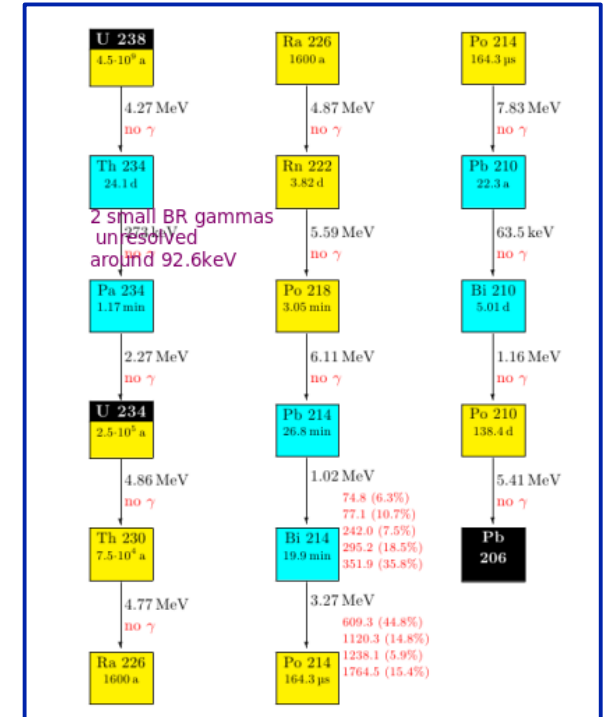
Monitoring Operations Parameters

- Remote monitoring (incl. alarms) of operations parameters to ensure detector stability and data quality
 - Trigger rate 100-2700 keV
 - Dewar LN₂ level → weekly refills
 - GN₂ purge gas flow (4 slpm)
 - Bias voltage (4817±3) V
→ Energy ROI in MCA range
 - Leakage current
 - Room temperature & pressure



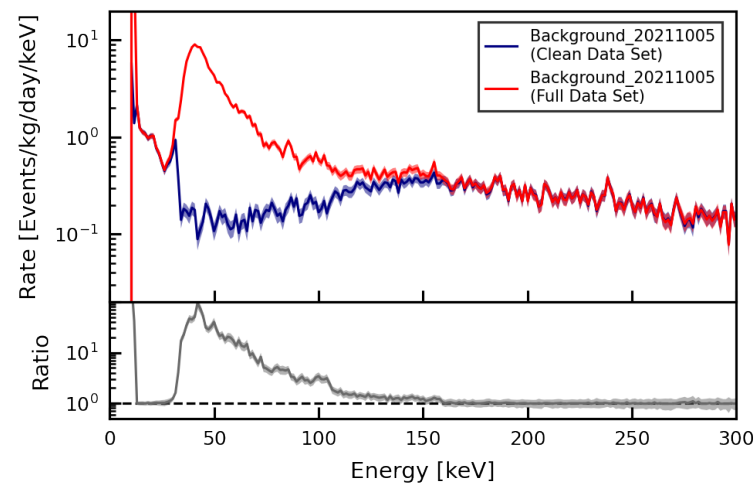
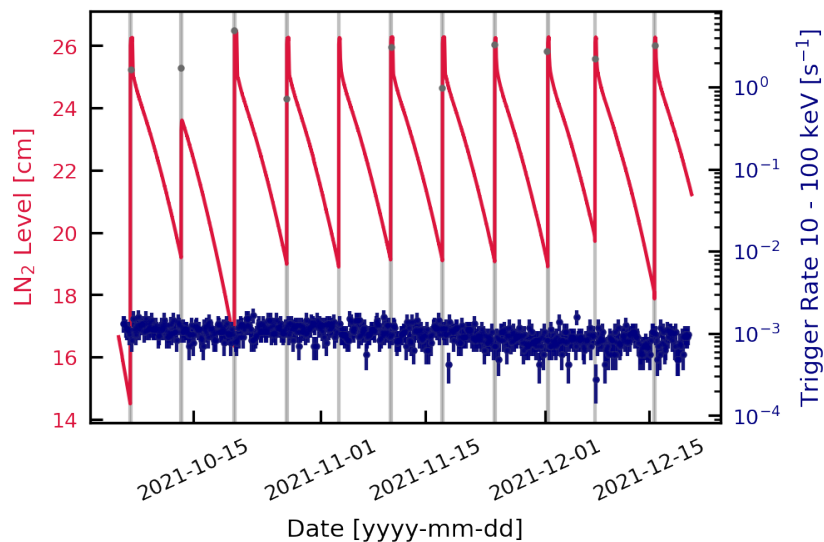
Background Contributions

- Low E (< 100 keV): electronic noise
- Higher E: detector & shielding materials, environmental radon
 - ^{238}U , ^{232}Th and ^{235}U found naturally in minerals, daughters from α/β -decays detected in whole detector range
 - Gaseous ^{222}Rn from ^{238}U chain from rock / water
 - ventilation, enclosure, GN_2 purge
 - traced via ^{214}Bi decays
 - ^{40}K (present in Earth mantle)
 - Cosmogenic ^{60}Co (in Cu shield and enclosure)
 - Anthropogenic ^{137}Cs



Reproducible Low-Energetic Noise

- Observed low-energetic noise, temporally correlated with LN₂ dewar refills, that might leak into the ROI (contributes for energies of up to ~ 150 keV)
- Unbiased removal of affected data sets based only on derivative of LN₂ level



The Pauli-Exclusion-Principle (PEP)



Wolfgang Pauli

- Two or more identical fermions cannot occupy the same quantum state within a quantum system simultaneously
- Example: (n, l, m_l, m_s) for electrons in atoms
- Concerning the exchange of two identical particles, the total wave function is antisymmetric (symmetric) for fermions (bosons) → different statistics

The *New* Electron Conundrum

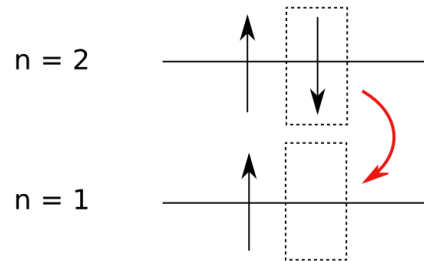
- Categorize experiments by how “new” the fermion-system interaction can be assumed to be
 - **Type I:** fermion has not previously interacted with any other fermions
 - primordial system formation
 - recently created fermions e.g. from β decay or pair production (Type Ia)
 - **Type II:** fermion has not previously interacted with that investigated system
 - distant fermions brought to interact with system e.g. Ramberg-Snow technique
 - nearby fermions brought to interact with system e.g. electrons in the Fermi sea of a conductor (Type IIa)
 - **Type III:** fermion within investigated system
 - violate the Messiah-Greenberg superselection rule

The New Electron Conundrum

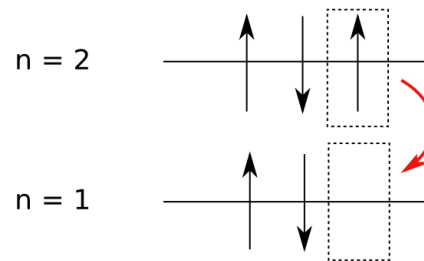
Process	Type	Experimental limit	$\frac{1}{2}\beta^2$ limit	Reference
Atomic transitions				
$\beta^- + \text{Pb} \rightarrow \check{\text{Pb}}$	Ia		3×10^{-2}	[23]
$e_{pp}^- + \text{Ge} \rightarrow \check{\text{Ge}}$	Ia		1.4×10^{-3}	This work
$e_I^- + \text{Cu} \rightarrow \check{\text{Cu}}$	II		1.7×10^{-26}	[48]
$e_I^- + \text{Cu} \rightarrow \check{\text{Cu}}$	II		4.5×10^{-28}	[8]
$e_I^- + \text{Cu} \rightarrow \check{\text{Cu}}$	II		6.0×10^{-29}	[9]
$e_I^- + \text{Pb} \rightarrow \check{\text{Pb}}$	II		1.5×10^{-27}	This work
$e_I^- + \text{Pb} \rightarrow \check{\text{Pb}}$	IIa		2.6×10^{-39}	This work
$\text{I} \rightarrow \check{\text{I}} + \text{X-ray}$	III	$\tau > 2 \times 10^{27}$ sec	3×10^{-44}	[49]
$\text{I} \rightarrow \check{\text{I}} + \text{X-ray}$	III	$\tau > 4.7 \times 10^{30}$ sec	6.5×10^{-46}	[13]
Nuclear transitions				
$^{12}\text{C} \rightarrow ^{12}\check{\text{C}} + \gamma$	III	$\tau > 6 \times 10^{27}$ y	1.7×10^{-44}	[38]
$^{12}\text{C} \rightarrow ^{12}\check{\text{C}} + \gamma$	III	$\tau > 4.2 \times 10^{24}$ y		[3]
$^{12}\text{C} \rightarrow ^{12}\check{\text{C}} + \gamma$	III	$\tau > 5.0 \times 10^{31}$ y	2.2×10^{-57}	[11]
$^{12}\text{C} \rightarrow ^{12}\check{\text{C}} + \gamma$	III	$\tau > 4.6 \times 10^{26}$ y	2.3×10^{-57}	[51]
$^{16}\text{O} \rightarrow ^{16}\check{\text{O}} + \gamma$	III	$\tau > 4.6 \times 10^{26}$ y		[3]
$^{12}\text{C} \rightarrow ^{12}\check{\text{N}} + \beta^- + \bar{\nu}_e$	IIIa	$\tau > 3.1 \times 10^{24}$ y		[11]
$^{12}\text{C} \rightarrow ^{12}\check{\text{N}} + \beta^- + \bar{\nu}_e$	IIIa	$\tau > 3.1 \times 10^{30}$ y		[11]
$^{12}\text{C} \rightarrow ^{12}\check{\text{N}} + \beta^- + \bar{\nu}_e$	IIIa	$\tau > 0.97 \times 10^{27}$ sec	6.5×10^{-34}	[35]
$^{12}\text{C} \rightarrow ^{12}\check{\text{B}} + \beta^+ + \nu_e$	IIIa	$\tau > 2.6 \times 10^{24}$ y		[3]

Found Phys 42, 1015–1030 (2012)

Normal...



Non-Paulian...



atomic 2p – 1s transition

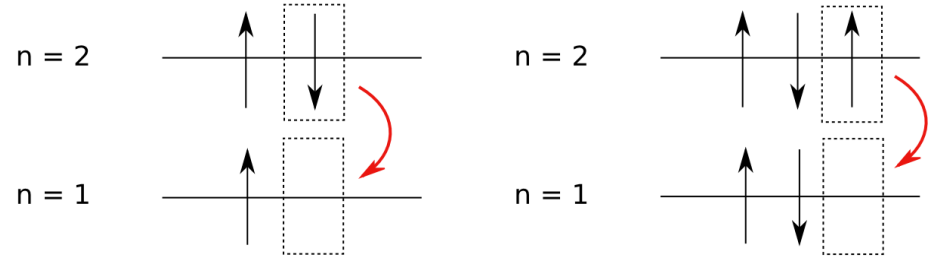
Atomic Theory

- Objective: capture of free electron onto atom via PEP violating process
- Capture probability:

$$\sigma_D = \sum_{n \geq 2} \frac{8\pi}{3\sqrt{3}} \frac{\alpha^5}{n^3} \frac{Z_{eff}^4}{K(K + E_n)}$$

→ $P_{cpt} = 0.009$ (0.058) for Pb (Cu)

- Cascade
- X-ray energies:
→ energy shifted down due to additional shielding of the nuclear charge



Transition	Cu		Ge		Pb	
	Forb.	Allow.	Forb.	Allow.	Forb.	Allow.
$1s-2p_{3/2} K_{\alpha 1}$	7741	8047	9543	9886	73713	74961
$1s-2p_{1/2} K_{\alpha 2}$	7723	8027	9516	9854	71652	72798
$2p_{3/2}-3s$	738		953		8920	
$2p_{1/2}-3d_{3/2}$	873	951	1131	1221	12241	12611
$2p_{3/2}-3d_{3/2}$	856	931	1104	1189	10180	10448
$2p_{1/2}-3s$	755		981		10981	
$2p_{3/2}-3d_{5/2}$	856	931	1104	1190	10276	10550

Found Phys 42, 1015–1030 (2012)

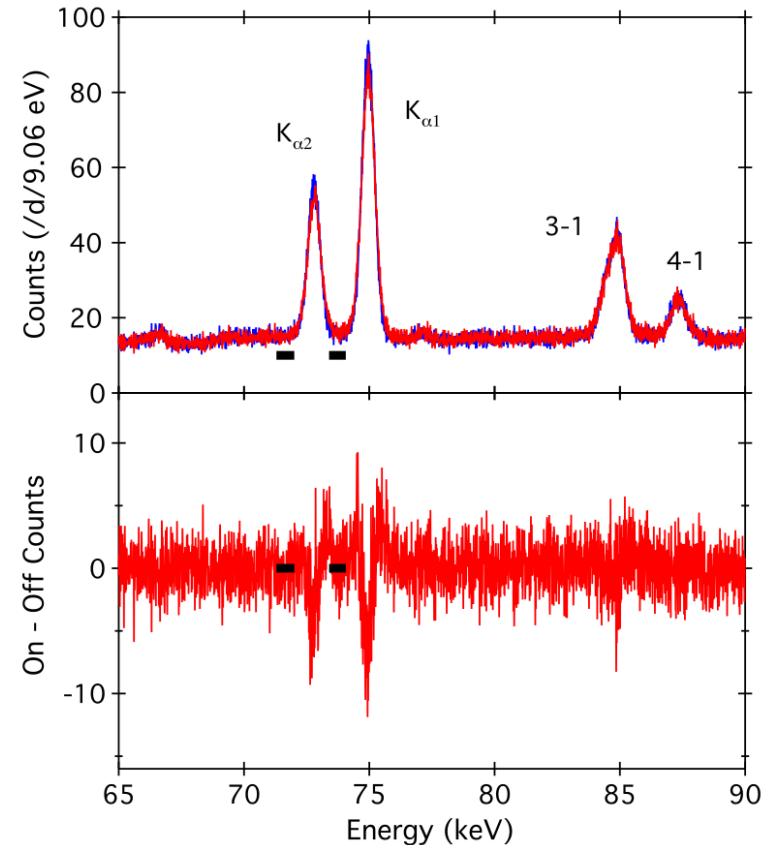
Energies in eV

The Experiments – Current Through Lead

- Ramberg-Snow concept → **Type II experiment**
- Compare current-on/off data in regions with minimal $\sqrt{B}/\epsilon_{\text{ROI}}$
- Increased width and background in current-on weakens constraint on $\frac{1}{2}\beta^2$
- Resulting 3σ upper limit:

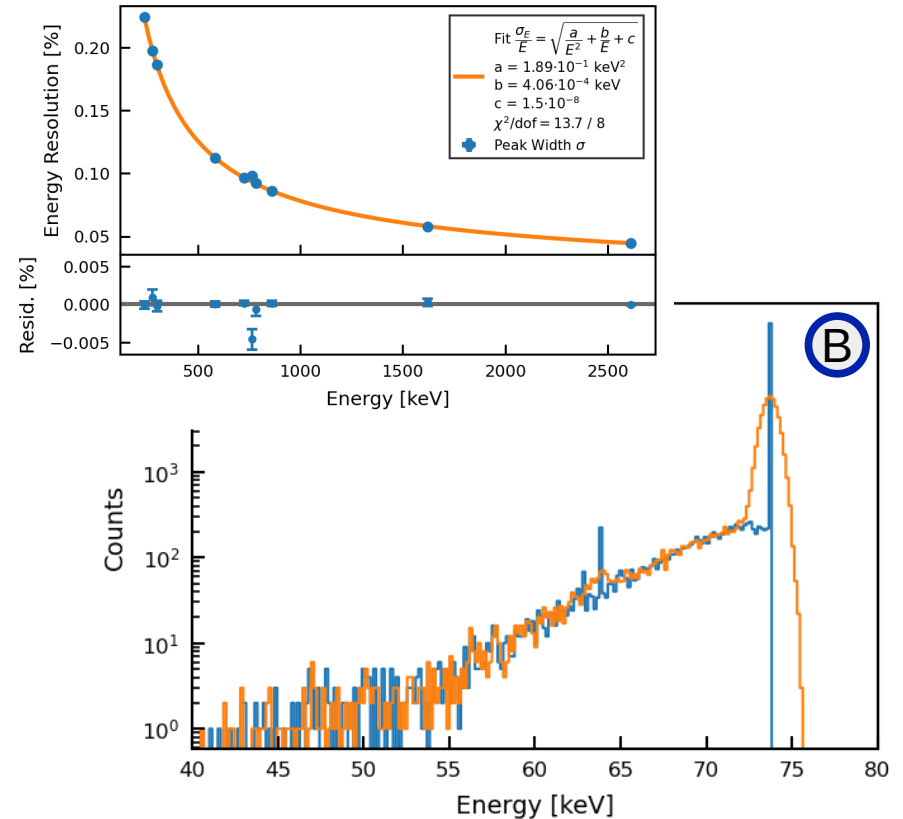
$$\frac{1}{2}\beta^2 < \frac{N_{3\sigma}}{N_{\text{new}}\epsilon_x P_{\text{cpt}} N_{\text{int}}} = 1.5 \times 10^{-27}$$

Found Phys 42, 1015–1030 (2012)



Geant4 Simulations

- Geant4 simulations with framework for sample efficiency simulations*
- Number of simulated gammas: $10^7 - 10^8$ (depending on thickness)
- Gamma energy: 73.713 keV (energy of PEP violating Pb $K_{\alpha 1}$)
- Reduced length (0.1 μm) and energy (250 eV) cuts in *PhysicsList*
- Energy-resolution smearing, binning according to Gator MCA



*https://github.com/Physik-Institut-UZH/Gator_2020

Electrical Connections

- Agilent 5761A high current supply (0-6V, 0-180A)
- High current DSUB (40 A/pin) connector in top plate
- Multiple cables for flexibility and heat dissipation
- Segmented OFHC Cu rod with PTFE insulation into sample chamber

